JAIST Repository
https://dspace.jaist.ac.jp/

Title	Modification for Uniform Surface of Nafion Ultra-thin Film Deposited by Inkjet Printing
Author(s)	Guo, Yanglu; Ono, Yutaro; Nagao, Yuki
Citation	Langmuir, 31(37): 10137-10144
Issue Date	2015-09-01
Type	Journal Article
Text version	author
URL	http://hdl.handle.net/10119/13804
Rights	This document is the Accepted Manuscript version of a Published Work that appeared in final form in Langmuir, copyright (c) American Chemical Society after peer review and technical editing by the publisher. To access the final edited and published work see http://pubs.acs.org/articlesonrequest/AOR-tqeB6XsQMhhKSpeYzDgy.
Description	

JAIST
JAPAN
ADVANCED INSTITUTE OF
SCIENCE AND TECHNOLOGY

Japan Advanced Institute of Science and Technology

Modification for Uniform Surface of Nafion Ultra-thin Film Deposited by Inkjet Printing

Yanglu Guo, Yutaro Ono, Yuki Nagao*

School of Materials Science, Japan Advanced Institute of Science and Technology,

1-1 Asahidai, Nomi, Ishikawa 923-1292

Abstract

A lack of knowledge about the features of Nafion confined to ultra-thin films at the interface has motivated additional examinations to promote the performance of polymer electrolyte membrane fuel cells (PEMFCs). In this work, we demonstrated the utilization of practical film-forming technique inkjet printing to fabricate a Nafion ultra-thin film less than 10nm thickness. However, the well-known "coffee-ring" effect caused poor quality of the printed pattern, which has restricted its application. This report describes a systematic investigation of necessary parameters such as ink concentration, substrate type, pitch, and offset for printing processes. Furthermore, post-treatment in an ethanol vapor atmosphere exhibited a significant effect on flattening and homogenizing the film surface morphology. Results show that the well-distributed Nafion ultra-thin film modified by ethanol vapor annealing manifested much-improved proton conductivity.

1. Introduction

With global growing concerns related to the environment and fossil fuel depletion, the exploration of green energy sources providing much higher efficiency and lower emissions has spurred a trend to development of clean power sources of generation. Numerous and diverse efforts have been made in recent decades to develop polymer electrolyte fuel cells (PEFCs) technologies to support this promising energy sources because of its distinct features such as high energy efficiency. Nafion, the most widely used proton conductor in PEFCs, is known for its excellent conductivity and thermal, mechanical stability.[1-3] As a product of the Dupont Chemical Co., Nafion is a perfluorosulfonated copolymer consisting of a hydrophobic perfluorocarbon backbone with attached polyether side chains terminated with a hydrophilic sulfonic acid group,[4-7] as presented in Figure 1.

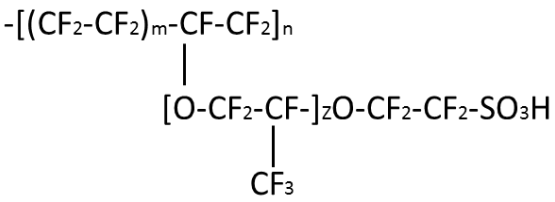

Figure 1. Nafion chemical structure

Extensive studies have been undertaken to investigate the proton conductivity of Nafion, which is crucially important for PEFCs performance. Proton conductivity depends on the level of hydration in the Nafion membrane. However, information is lacking about the structure and water transport mechanisms of Nafion confined to polyelectrolyte thin films at the interface, which incurs deviations in morphology, proton conductivity with that of bulk membrane properties.[8,9] Because triple-phase boundaries as the active sites within catalyst layer play a

critical role in electrochemical reactions, understanding the properties of thin polymer layer at triple-phase boundaries is a key point to facilitate the performance of PEFCs overall. Our research, particularly addressing interfacial confinement between thin polymer films and free surface substrate, contributes to greater insights into proper triple-phase boundaries, which is meaningful to promote PEMFCs performance.[10]

As a direct-patterning technique, inkjet printing possesses important advantages over spin coating and spraying methods.[11-13] Costs and waste can also be reduced because of the on-demand printable process.[14] Inkjet printing is an efficient, high-speed film-forming technique, with the capability of accurate ejection of a small amount of ink onto specific substrate locations through a tiny nozzle,[15] which enables fabrication of an ultra-thin film at a selective interface. Additionally, by ejecting a reproducible quantity of ink without physical contact with the pattern, this technique remarkably reduces contamination on the surface,[16-18] which gives it an important role in various applications for manufacturing devices such as fuel cell electrodes,[19-22] transistors, solar cell.[23] For this study, this innovative film-forming technique was selected for the printing process.

Figure S1 presents a schematic illustration of the printing process of single droplet and line pattern using inkjet printing. The single-droplet shape and size of depend on the substrate type, ink concentration, and drying behavior. For inkjet printing, the difference of timescale between evaporation and movement of solutes forms the well-known “coffee ring” effect, which might produce a differently morphological Nafion than in the case of spin coating and cast methods. Therefore, the comprehension of evaporation behavior is crucially important for control of the drying process and for suppression of the “coffee-ring” effect. The quality of the pattern produced by inkjet printing can be affected mainly by three important factors: printer conditions,

ink properties, and a substrate surface. The location and jetting configuration are determined by the printer. Ink properties such as viscosity and surface tension, and the wettability of a droplet on different types of substrate surface, are important determinants of the shape and size of the deposit.[24, 25]

However, the poor surface morphology of inkjet-printed films is caused mainly by the well-known “coffee-ring” effect. When a sessile drop dries on a solid surface, the faster evaporation at the contact line causes a capillary flow outward to the edge. This outward flow carries dispersed material to the edge and engenders aggregation at the contact line, as demonstrated by Deegan et al.[26] A few approaches have been investigated to suppress this undesired phenomenon, such as utilization of mixed solvent[27-29] and solvent vapor atmosphere,[30] addition of surfactants,[31, 32] optimization of drying temperature[33] and humidity.[14] However, most studies have emphasized the modification of a single droplet or line pattern; no information about the large printing size of ultra-thin film has been reported.

This work explores optimization of necessary parameters related to the printing process for fabricating Nafion ultra-thin film at the interface by inkjet printing has been proposed. We assessed a novel method to modify the surface morphology of ejected ultra-thin film under a saturated ethanol vapor atmosphere, which flattened the film surface with a uniformly distributed morphology. This technique enhances the proton conductivity of the Nafion ultra-thin film.

2. Experimental

2.1. Materials

5%-Nafion dispersion (DE521 CS type), 1-propanol, and 2-propanol were purchased from Wako Pure Chemical Industries Ltd. The quartz substrate was purchased from Sendai Sekiei glass factory, Japan. A high-resistivity Si wafer for the IR measurement was purchased from Electronics and Materials Co Ltd.

2.2. Ink solution preparation and wettability check

Four inkjet printing inks with different concentrations were prepared by diluting 5%-Nafion dispersion with 1-propanol. The concentrations are 0.29 wt% (ink A, 5%-Nafion : 1-propanol = 1:19 v/v), 0.18 wt% (ink B, 5%-Nafion : 1-propanol = 1:29 v/v), 0.14 wt% (ink C, 5%-Nafion : 1-propanol = 1:39 v/v) and 0.11 wt% (ink D, 5%-Nafion : 1-propanol = 1:49 v/v). Three quartz and Si substrates were prepared with different pretreatments: as-received quartz (substrate A), as-received Si (substrate D), washed by 2-propanol quartz (substrate B), washed by 2-propanol Si (substrate E), treated by plasma treatment quartz (substrate C), and treated by plasma treatment Si (substrate F). Plasma treatment was conducted by a vacuum plasma system (Cute-MP; Femto Science, Korea). To investigate the surface hydrophilicity of these three substrates, 20 μL of sessile water or ink A droplet by micropipette was placed onto each substrate (substrates A, B, C, D, E, and F) to compare the wettability.

2.3. Fabrication process by inkjet printing

A commercial drop-on-demand mode piezoelectric inkjet printer (LaboJet-500; Microjet Corp.) was used. It was equipped with a single nozzle (IJHB-300) with diameter of around 150 μm and a nominal ejected droplet volume of 150–700 pL. This nozzle ejected inks onto the substrate with distance of around 2 mm. The droplet speed was measured using a droplet observation system with an LED strobe, stage controller, and HCS+ program. The ink-jet speed was

optimized at 5 m s^{-1}**.** The optimal jetting frequency was 500 Hz. To fabricate the best quality of Nafion ultra-thin film, the optimization of pitch and offset length for the deposition is vitally indispensable. The pitch is the distance between the centers of two droplets parallel to the inkjet scanning direction (line direction). The offset is the distance between two jetted lines. A single droplet with no overlap was obtained instead of a continuous line if the pitch increases to a value larger than droplet diameter. Each single scanned line will be obtained rather than the overlapped line patterns which can ultimately form a pattern of film if the offset increases to a value larger than the width of line. Therefore the optimal pitch and offset length are prerequisites for film fabrication.

2.4. Film modification by ethanol vapor atmosphere

Ethanol vapor was applied to modify the surface morphology and smoothness of Nafion ultra-thin film with considerable roughness. A printed size of 5 × 5 mm^2 Nafion ultra-thin film on the substrate D was treated for 5min in a Petri dish saturated with an ethanol vapor atmosphere.

2.5. Film surface morphology and thickness measurement

Optical microscope (BX-51; Olympus Corp.) was used to examine the surface morphology of the printed pattern. An atomic force microscope (AFM, Nanoscope IIIa; Veeco) with tapping mode was used to investigate the surface morphology and thin film roughness. Silicon cantilevers (SI-DF3FM; Nanosensors Corp.) with a spring constant between 2.8 N m^{-1} and 4.4 N m^{-1} and a resonance frequency of 79–89 kHz. The measurements were taken under an air atmosphere with a scan rate of 0.4 Hz and a scanned area of 1×1 μm^2. An AFM (VN-8000; Keyence Co.) equipped with DFM/SS mode cantilever (OP-75041; Keyence Co.) was applied to measure the film thickness.

2.6. Proton conductivity measurement

Impedance measurements of ejected Nafion ultra-thin film on substrate A were taken in the relative humidity (RH) of 40–95% using an impedance/gain-phase analyzer (SI1260; Solartron Analytical) and a dielectric interface system (1296; Solartron Analytical) to investigate proton transport properties. A humidity and temperature controlled chamber (SH-221; Espec Corp.) was used for RH and temperature controlling.[10] For impedance measurements for Nafion ultra-thin films, a two-probe system was used. The electrode configuration was in the plane parallel to the substrate surface to procure measurements of the current flow. The Au paste used for the electrode was located parallel at the edge of the thin film. The impedance data were gathered up in the frequency range of 1–10 MHz with amplitude of 50 mV. Proton conductivity (σ) was calculated as:

$$\sigma = \frac{d}{RLt} \quad (1)$$

where d stands for the distance between the electrodes; R denotes the resistance value; L signifies the length of electrodes; and t represents the thin film thickness. The reproducibility was checked more than three times. The error is estimated within ± 0.1 log (σ / S cm^{-1}).

3. Results and discussion

Figures 2(a, b, c), respectively portray water droplet images from the top and side views for each substrate (substrates A, B, and C). Substrate C exhibits a more hydrophilic surface rather than either substrate A or B. These differences in the hydrophilicity of the substrate surface were explained in our previous report.[34] Figures 2(d, e, f) shows ink A (Nafion solution, not water) droplet images from the top and side views for each substrate (substrates A, B, and C). The contact angle of the ink A droplet shows an opposite trend to that of the water droplet shown in

Table 1. The ink A droplet spreads freely on the surface of substrate A (as-received quartz substrate), although it exhibits much higher contact angle in the case of substrate C (plasma treated). To elucidate whether this reverse trend derives from structural properties of Nafion, we investigated the contact angle of the solvent itself (1-propanol) without containing Nafion. Figures 2(g, h, i) show solvent droplet images from the top and side views for each substrate (substrates A, B, and C). The contact angle shows a similar trend in the case of the water droplet as presented in Figures 2(a, b, c). The ink solvent itself has better affinity to substrate C than to substrate A. These results indicate that the wettability of Nafion mixed solution has particular affinity to the quartz substrate. This characteristic affinity might be attributable to the amphipathic Nafion structure, which comprises the nonpolar perfluoroethylene backbone and polar perfluoroether side chains terminated with sulfonic acid groups. The same trails of water and ink A droplet on substrate D, E, and F were compared as shown in Figures S2 and Table S1. The Nafion mixed solution presented the lowest contact angle on substrate D (as-received Si), which shows similar results to those obtained for the case of substrate A (as-received quartz).

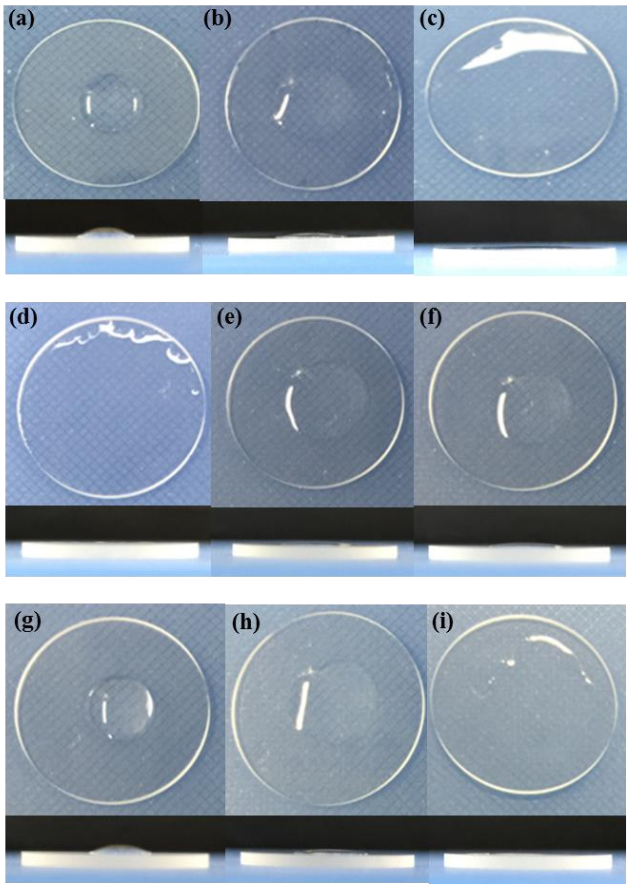

Figure 2. Top and side views (a, b, c) respectively depict 10 μL of sessile water droplet on substrates A, B, and C. In contrast, 10 μL of ink A dropped respectively on substrates A, B, and C (d, e, f) exhibited reverse wettability compared with the water droplet on the same substrate. 10~~20~~ μL of solvent itself dropped respectively on substrates A, B, and C (g, h, i).

Table 1. Contact angle measurement on the quartz substrate

	Substrate A	Substrate B	Substrate C
Water droplet	35°	30°	＜5°
Ink A (Nafion mixed solution)	＜5°	23°	28°
1-propanol	30°	20°	＜5°

Ink A was ejected onto each substrate by inkjet printing to check the spread diameter of the dried single droplet as shown in Table 2. The largest single-droplet diameter is achieved for substrate A. The smallest is for substrate C. This result shows the same result with the case of droplet by micropipette. Spreading of the larger area for the droplet demonstrates that the Nafion solution has a higher affinity to the more hydrophobic surface, substrate A. The ink concentration is another necessary factor for the printing and drying process. As shown in Table 1, lower ink concentration engenders larger drop diameter because of the lower ink viscosity. Interestingly, the droplet diameter does not change so much in the range of our experimental concentration (between ink A and ink D), as shown in Table 2. Along with the decreasing ink concentration, the drop contact line becomes much thinner than before, as shown in Figure S3. To quantify this variation, the surface profile was applied to measure the contact line thickness, as shown in Table 3. This result demonstrates a high concentration of ink ejected onto plasma treated substrate, the "coffee-ring" effect will be aggravated. Therefore, to improve the quality of printed pattern, the as-received substrate and low ink concentration were chosen to proceed with the next step of the printing process: film-forming.

Table 2. Average diameter of single droplet with varying concentrations of Nafion ejected on quartz substrate surfaces of three types.

	Nafion concentration	As-received quartz substrate	2-propanol washed quartz substrate	Plasma-treated quartz substrate
Ink A	0.29 wt%	365 μm	318 μm	281 μm
Ink B	0.18 wt%	377 μm	326 μm	296 μm
Ink C	0.14 wt%	380 μm	339 μm	313 μm
Ink D	0.11 wt%	396 μm	345 μm	326 μm

Table 3. Contact line thickness of the single droplet with varying concentration of Nafion ejected on quartz substrates of three types.

	Nafion concentration	As-received quartz substrate	2-propanol washed quartz substrate	Plasma treated quartz substrate
Ink A	0.29 wt%	30–55 nm	48–70 nm	75–100 nm
Ink B	0.18 wt%	15–30 nm	30–68 nm	40–70 nm
Ink C	0.14 wt%	15–25 nm	30–55 nm	40–58 nm
Ink D	0.11 wt%	15–20 nm	30–45 nm	35–50 nm

Pitch (dot-to-dot distance) and offset (line-to-line distance) for inkjet printing are pivotal parameters for the film fabrication. A continuous line was formed when the droplets were overlapped, as shown in Figure S4. Microscope images show that pinning occurs at the three-phase boundary during printing the line,[27] and becomes much heavier with a smaller pitch of 180

μm, as shown in Table 4. The smaller dot-to-dot distance caused a larger part of single droplet overlapping mutually, which forced more matter to move to the edges and which ultimately formed a larger width of line pattern with heavier and straighter edges. With lower edge-to-center height ratio, the pitch of 335 μm was selected as the next experiment: film-forming.

Table 4. Thickness of the edges and edge-to-center height ratio of line pattern with different pitch on the substrate A using the concentration of Nafion / 1-propanol = 0.11 wt%.

Pitch	Thickness at the edge	Thickness at the center	Edge-to-center height ratio(*he / hc*)
180 μm	40-55 nm	18-25 nm	2.2
335 μm	15-22 nm	10-15 nm	1.5

A continuous film was formed when each dotted line was overlapped, as shown in Figure S5. However, the boundaries were apparent at the overlaid parts. The height of boundaries formed by different offset lengths is shown in Table 5. The offset of 315 μm was found to be the upper limit; otherwise a discontinuous film would be produced. However, as the pitch increases, some bulges with much greater thickness on the boundaries emerge, as shown in Figure 3(a). It was assumed that the pressure difference caused the pumping of the ink from the bulge to the ridge.[35, 36] However, the optimization of pitch and offset might ineffectively diminish the thickness difference between boundaries and the center part of film. This poor quality of wavy-like surface morphology seems unavoidable based on the theory of film-forming by inkjet printing, which restricts the ejected ultra-thin film to a more extensive application. Therefore, modification of the film surface morphology becomes an urgent mater to be resolved.

Table 5. Thickness at non-boundary places and boundaries with different offset

	Thickness at the non-boundary places	Thickness at boundaries
Pitch=335 μm Offset=180 μm	15-30 nm	70-100 nm
Pitch=335 μm Offset=315 μm	4-7 nm	20-50 nm

In this study, to obtain smoother and more uniform surface morphology of Nafion ultra-thin film, a novel method is demonstrated with no surfactant additives and pre-modified substrate. Modification for the smooth surface morphology was simply conducted using solvent vapor annealing and rapidly drying process. The experimental is presented in Movie 1. The ultra-thin film with the boundaries was treated in saturated ethanol vapor atmosphere in a Petri dish. During the treatment period, it was observed that ethanol vapor adsorbed rapidly onto the surface of Nafion ultra-thin film and Si wafer. The boundaries were recognized clearly as shown in Figure 3(b). After treatment in ethanol vapor for a few minutes, the boundaries disappeared immediately with the evaporation of ethanol vapor when exposed to air vapor by unfolding the lid of the Petri dish, as shown in Figure 3(c). (see Movie 1).

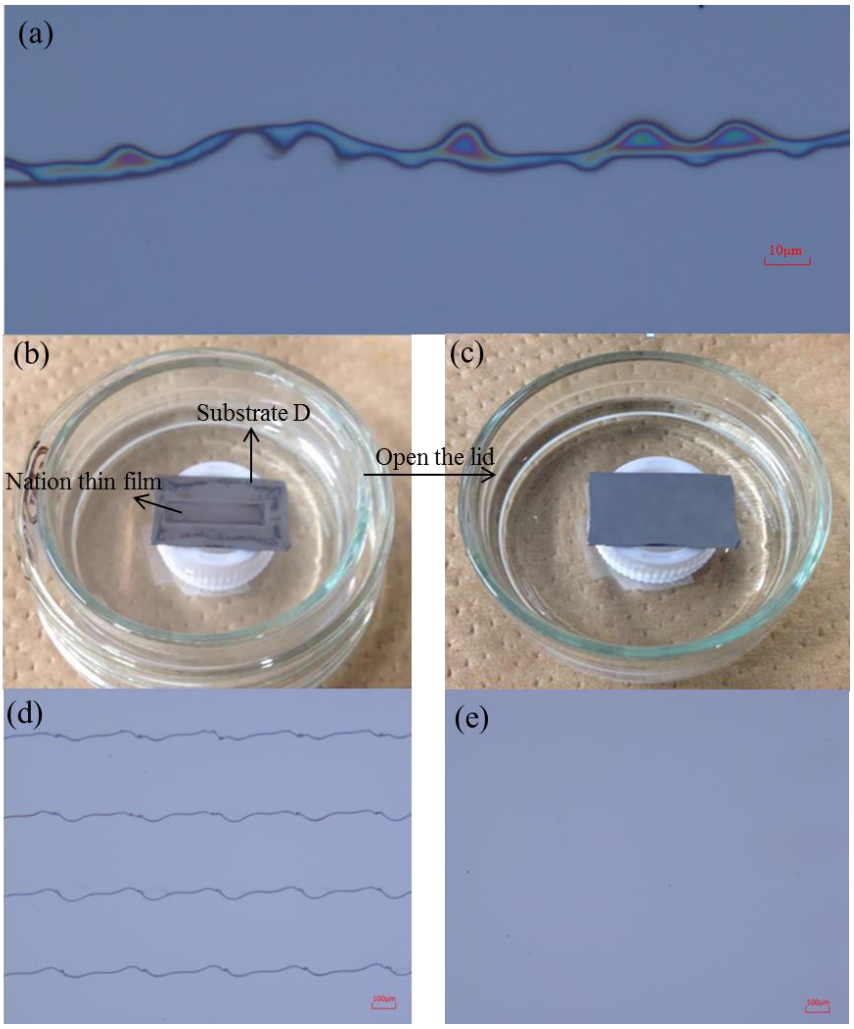

Figure 3. (a) Optical microscopic image of bulges on boundaries in ejected Nafion thin film on substrate A with the concentration of Nafion /1-Propanol as 0.11 wt%. (b) Photograph of ejected Nafion ultra-thin film on substrate D treated in a Petri dish under saturated ethanol vapor atmosphere for 5 min. During the treatment process, ethanol vapor adsorbed onto the substrate and film, which made the boundaries more visible (See Movie 1). (c) After opening the lid, all boundaries disappeared with the evaporation of ethanol vapor. (d) Optical microscopic image of Nafion ultra-thin film without ethanol vapor treatment. (e) Optical microscopic image of Nafion ultra-thin film after ethanol vapor treatment.

Optical microscopic images of Nafion ultra-thin film ejected on substrate D with printing size of 5×5 mm^2 is shown in Figure 3(d). Boundaries appearing in film that had been treated in air without ethanol vapor annealing existed at the distance of a line width. In sharp contrast, an empty image with no trace of boundary was obtained as shown in Figure 5, which shows that ethanol vapor annealing has a strong ability of flattening the surface of Nafion ultra-thin film.

The surface morphology of Nafion ultra-thin film was measured using atomic force microscopy (AFM). Figures 4(a) and 4(b) present AFM images at the area without boundaries of Nafion ultra-thin film before ethanol solvent annealing. A rough surface image was obtained and the roughness was 1.3 nm. In contrast, much more uniform and smoother surface morphology was obtained after the ethanol and air treatments as portrayed in Figure 4(c) and 4(d). The surface roughness was reduced to 0.9 nm height. Figure 4(e) and 4(f) present the AFM images at the area with one boundary of Nafion ultra-thin film before ethanol solvent annealing. This boundary with bulges was observed at many places on the surface and the average height is ca. 200 nm. However, these high boundaries at every location (5×5 mm^2) on the surface disappeared after the ethanol and air treatments as portrayed in Figure 4(g) and 4(h). Results showed that smooth and uniform surface morphology of Nafion ultra-thin film in the molecular level was obtained with no surfactant additives and pre-modified substrate. This flat and smooth Nafion ultra-thin film was achieved on the surface of as-received quartz substrate as well.

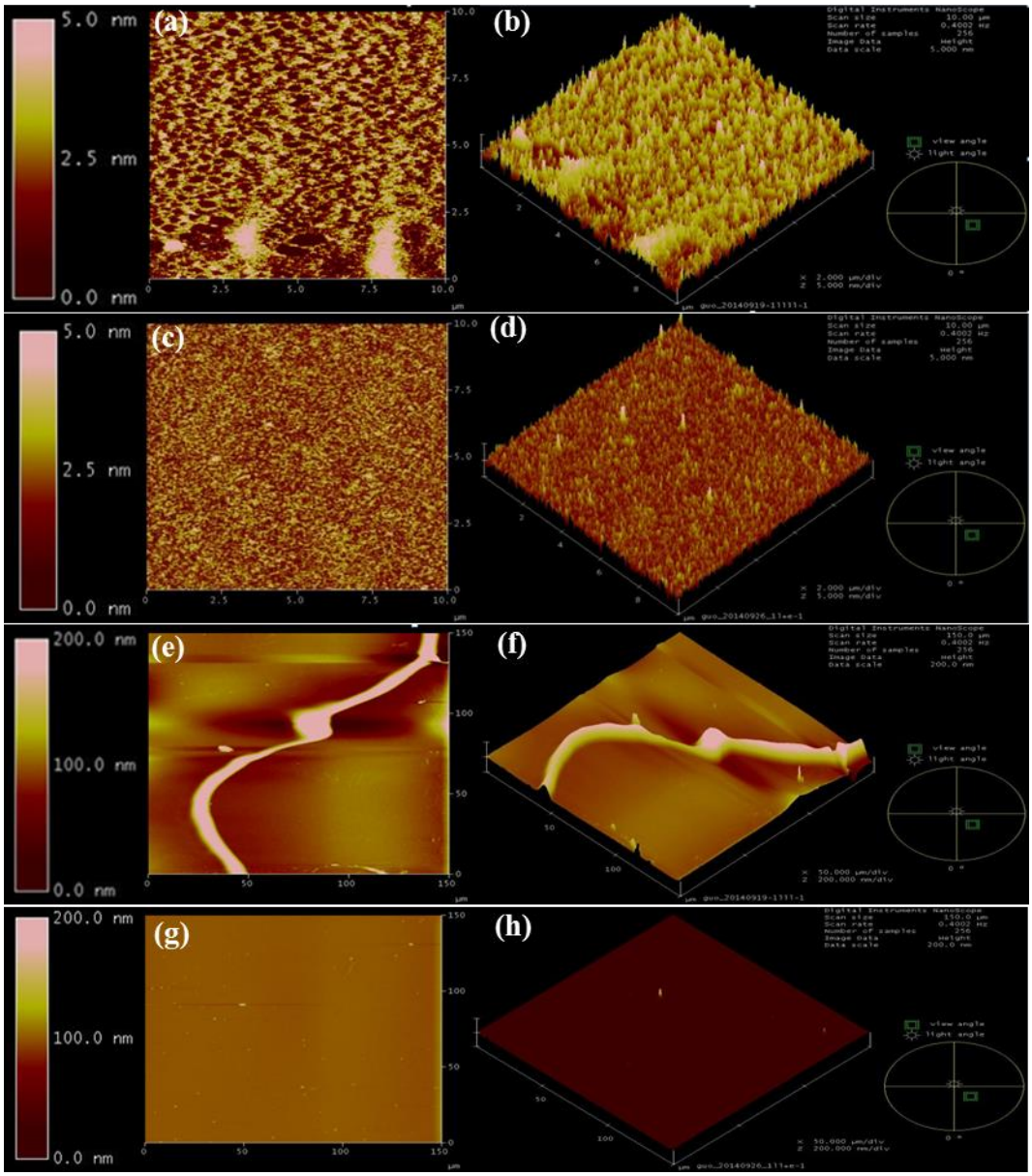

Figure 4. Tapping mode of atomic force microscope (AFM) images of Nafion thin film at the area without boundaries: (a, b) air vapor treated Nafion thin film with the surface of cell-like cavities and unevenness; (c, d) ethanol vapor treated Nafion thin film with a smoother and more uniform surface morphology; (e, f) air vapor treated Nafion thin film with a high thick boundary; and (g, h) ethanol vapor treated Nafion thin film with no boundaries in the film.

A possible reason for this interesting phenomenon might be the thickness change after ethanol vapor treatment, but the mechanism and reason for boundaries reappearance after closing petri dish (See movie 1) are still under investigation. From this result, it was identified that the ethanol vapor atmosphere owned the ability of flattening the film surface and homogenizing Nafion to uniform distribution.

Understanding Nafion interface is necessary to improve the fuel cell power and efficiency. Recently comparison of the lower proton conductivity at the Nafion interface to that of the bulk membrane has been reported.[10, 37-41] Additional research particularly addressing the interfacial confinement between thin polymer films and the free surface substrate is necessary to gain more insight into proper triple-phase boundaries, which is critically important to promote the performance of PEMFCs. The known fabrication of the Nafion ultra-thin film was used by spin coating and self-assembled technique.[10, 42] A normal Nafion ultra-thin film by inkjet printing has a considerable roughness by coffee-ring effect. This ultra-thin film did not yield reproducible impedance results for proton conductivity, perhaps because of the inconstant thickness. Using results of this study, we prepared the uniform 7-nm-thick Nafion ultra-thin film using ethanol vapor annealing. Impedance measurements were conducted and were found to be well reproducible. Figure 5 presents the proton conductivity dependence on the relative humidity. The proton conductivity of the inkjet ultra-thin film is one order of magnitude lower than that of the bulk membrane.[43] Comparing the case of the thin films on the quartz substrate, the proton conductivity by Modestino *et al.* is a half order of magnitude higher than that of our inkjet ultra-thin film.[37] They described that the hydrophilicity of the thin film surface can be altered by heat treatment and proton conductivity, which exhibits different values before and after the treatment. Figure 6 presents results of the hydrophilicity check for our 7-nm-thick film. Compared to the

hydrophilicity of the as-prepared thin film (Figure 6(a)), our ultra-thin film surface is more hydrophobic after impedance measurements under the humidified condition, as depicted in Figure 6(c). Roughness of the ultra-thin film surface was found to increase from 0.9 to 1.4 nm (Figure S7(b,c) in Supporting Information) after impedance measurements. Presumably, the water vapor affects the ultra-thin film surface, which becomes a more uniform and hydrophilic surface (Figure 6(d)) by the ethanol vapor treatment, showing decreasing roughness from 1.4 to 0.8 nm (Figure S7(d) in Supporting Information). This second treatment improves the proton conductivity much more than the case of the first ethanol treatment. The obtained proton conductivity is close to the value by Modestino *et al.* under a high RH condition. However, the proton conductivity dropped during impedance measurements with decreasing RH. This conductivity drop might be related with the structural change. The hydrophilicity changes by the water vapor annealing under 298 K as depicted in Figure 6(c). This further improvement of proton conductivity underscores the efficiency of ethanol vapor treatment for surface modification. The reproducibility and controllability by ethanol vapor treatment exhibit a unique superiority in surface modification, which might broaden its practical benefits in many engineering fields.

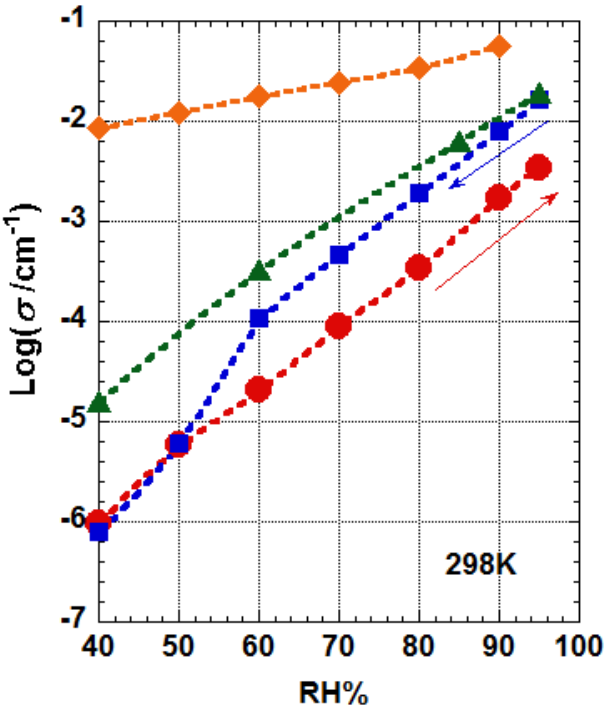

Figure 5. Relative humidity dependence of proton conductivity for the Nafion ultra-thin films: (●) 7 nm thick film treated by ethanol vapor, (■) 7 nm thick film by the second ethanol vapor treatment after the first conductivity measurement under humidified condition, (▲) 10-nm-thick Nafion thin film reported by Modestino *et al*,[37] and (♦) Nafion 117 bulk membrane.[43]

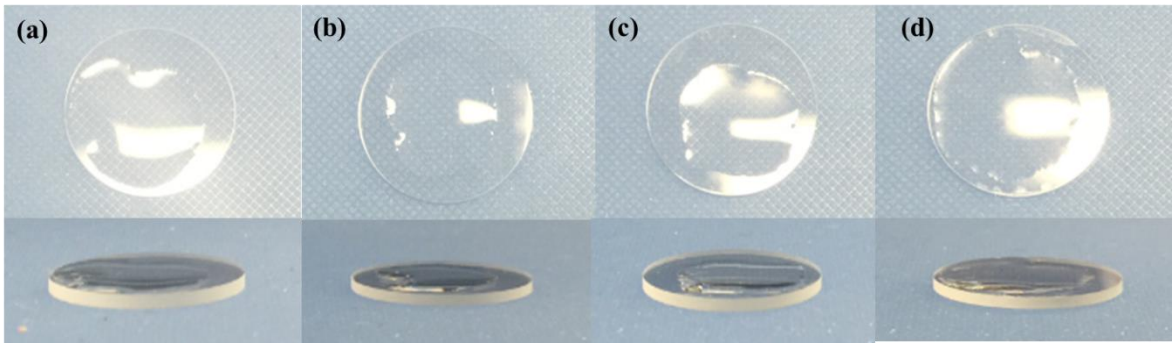

Figure 6. Hydrophilicity check (20μL of water drop) for the Nafion ultra-thin film: (a) as-prepared, (b) after ethanol vapor treatment, (c) after conductivity measurements under humidified conditions, and (d) after repeated ethanol vapor treatment.

4. Conclusions

A Nafion ultra-thin film with greatly enhanced quality has been fabricated using inkjet printing technique through optimization of three important parameters: ink concentration, substrate type, and length of pitch and offset. During the post-treatment process, the ethanol vapor annealing demonstrated a remarkable effect on surface modification, suppressing the “coffee-ring” effect derived from the operating mechanism of inkjet printing and the evaporation process. This novel treatment not only fattened and homogenized the surface morphology of Nafion ultra-thin film with good reproducibility; it also accelerated the proton conductivity. This is the first time to propose a systematic approach for surface modification with a scale of ultra-thin film fabricated by inkjet printing, which demonstrates an admirable strategy to achieve well-distributed Nafion ultra-thin film and to broaden the applications for inkjet-printed patterns.

Acknowledgements

We thank JiuYang Zhang for editing the movie. This work was supported by the Japan Society for the Promotion of Science (JSPS) through the Funding Program (GR060) for Next Generation World-Leading Researchers (NEXT Program), initiated by the Council for Science and Technology Policy (CSTP). This work was partially supported by research funds of the Research Foundation for the Electrotechnology of Chubu (REFEC).

Supporting information

Schematic illustration of inkjet experimental, top and side views of water droplets on modified substrates, contact angle, optical microscope images of single-drop and single-line patterns,

surface morphology by AFM, and an experimental movie for the ethanol vapor treatment. This material is available free of charge via the internet at http://pubs.acs.org.

Author information

Corresponding author

*ynagao@jaist.ac.jp Phone: +81(Japan)-761-51-1541, Fax: +81(Japan)-761-51-1149, Address: 1-1 Asahidai, Nomi, Ishikawa 923-1292, Japan

Notes

The authors declare no competing financial interest.

References

(1) Springer, T. E.; Zawodzinski, T. A.; Gottesfeld, S. Polymer Electrolyte Fuel Cell Model. *J. Electrochem. Soc*. **1991**, *138*, 2334-2342.

(2) Kreuer, K. D. On the Development of Proton Conducting Polymer Membranes for Hydrogen and Methanol Fuel Cell. *J. Membr. Sci*. **2001**, *185*, 29-39.

(3) Mauritz, K. A.; Moore, R. B. State of Understanding of Nafion. *Chem. Rev.* **2004**, *104*, 4535-4585.

(4) Grodzinki, J. J. Polymeric Materials for Fuel Cells: Concise Review of Recent Studies. *Polym. Adv. Technol*. **2007**, *18*, 785-799.

(5) Hsu, W. Y.; Gierke, T. D. Ion Transport and Clustering in Nafion Perfluorinated Membranes. *J. Membr. Sci.* **1983**, *13*, 307-326.

(6) Peighambardoust, S. J.; Rowshanzamir, S.; Amjadi, M. Review of the Proton Exchange Membranes for Fuel Cell Applications. *Int. J. Hydrogen Energy* **2010**, *35*, 9349-9384.

(7) Jang, S. S.; Molinero, V.; Cagin, T.; Goddard III，W. A. Nanophase-segregation and Transport in Nafion 117 from Molecular Dynamic Simulation: Effect of Monomeric Sequence. *J. Phys. Chem. B* **2004**, *108*, 3149-3157.

(8) Eastman, S. A.; Kim, S.; Page, K. A.; Rowe, B. W.; Kang, S. H.; Soles, C. L. Effect of Confinement on Structure, Water Solubility, and Water Transport in Nafion Thin Films. *Macromolecules* **2012**, *45*, 7920-7930.

(9) Dishari, S. K.; Hickner, M. A. Confinement and Proton Transfer in Nafion Thin Films. *Macromolecules* **2013**, *46*, 413-421.

(10) Nagao, Y. Highly Oriented Sulfonic Acid Groups in a Nafion Thin Film on Si Substrate. *J. Phys. Chem. C* **2013**, *117,* 3294-3297.

(11) Lee, M. W.; Ryu, G. S.; Lee, Y. U.; Pearson, C.; Petty, M. C.; Song, C. K. Control of Droplet Morphology for Inkjet-printed TIPS-pentacene Transistors. *Microelectronic Engineering* **2012**, *95*, 1-4.

(12) Sirringhaus, H.; Kawase, T.; Friend, R. H.; Shimoda, T.; Woo, E. P. High-resolution Inkjet Printing of all-polymer Transistor Circuits. *Science* **2000**, *290,* 2123-2126.

(13) Kawase, T.; Moriya, S.; Newsome, C. J.; Shimoda, T. Inket Printing of Polymeric Field-Effect Transistors and its Applications. *Jpn. J. Appl. Phys.* **2005**, *44*, 3649-3658.

(14) Fukuda, K.; Sekine, T.; Kumaki, D.; Tokito, S. Profile Control of Inkjet Printed Silver Electrodes and Their Application to Organic Transistors. *Appl. Mater. Interfaces* **2013**, *5*, 3916-3920.

(15) Hopkins, A. R.; Straw, D. C.; Spurrell, K. C. Influence of Surface Chemistry on Inkjet Printed Carbon Nanotubes Film. *Thin Solid Films* **2011**, *520*, 1541-1545.

(16) Weng, B.; Liu, X.; Shepherd, R.; Wallace, G. G. Inkjet Printed Polypyrrole/collagen

Scaffold: A Combination of Spatial Control and Electrical Stimulation of PC12 Cells. *Synthetic Metals* **2012**, *162*, 1375-1380.

(17) Calvert, P. Inkjet Printing for Materials and Devices. *Chemistry of Materials* **2001**, *13*, 3299-3305.

(18) Weng, B.; Shepherd, R. L.; Crowley, K.; Killard, A. J.; Wallace, G. G. Printing Conducting Polymers. *Analyst* **2010**, *135*, 2779-2789.

(19) Taylor, A. D.; Kim, E. Y.; Humes, V. P.; Kizuka, J.; Thompson, L. T. Inkjet Printing of Carbon Supported Platinum 3-D Catalyst Layers for Use in Fuel Cells. *J. Power Sources* **2007**, *171*, 101-106.

(20) Towne, S.; Viswanathan, V.; Holbery, J.; Rieke, P. Fabrication of Polymer Electrolyte Membrane Fuel Cell MEAs Utilizing Inkjet Print Technology. *J. Power Sources* **2007**, *171*, 575-584.

(21) Saha, M. S.; Malevich, D.; Halliop, E.; Pharoah, J. G.; Peppley, B. A.; Karan, K. Electrochemical Activity and Catalyst Utilization of Low Pt and Thickness Controlled Membrane Electrode Assemblies. *J. Electrochem. Soc.* **2011**, *158*, 562-567.

(22) Shukla, S.; Domican, K.; Karan, K.; Bhattacharjee, S.; Secanell, M. Analysis of Low Platinum Loading Thin Polymer Electrolyte Fuel Cell Electrodes Prepared by Inkjet Printing. *Electrochim. Acta* **2015**, *156*, 289-300.

(23) Liang, Y. N.; Lok, B. K.; Wang, L.; Feng, C. G.; Lu, A. C. W. Effects of the Morphology of Inkjet Printed Zinc Oxide (ZnO) on Thin Film Transistor Performance and Seeded ZnO Nanorod Growth. *Thin Solid Films* **2013**, *544*, 509-514.

(24) Mabrook, M. F.; Pearon, C.; Jombert, A. S.; Zeze, D. A.; Petty, M. C. The Morphology, Electrical Conductivity and Vapour Sensing Ability of Inkjet-printed Thin Films of Single-wall

Carbon Nanotubes. *Carbon* **2009**, *47*, 752-757.

(25) Percin, G.; Khuri-Yakub, B. T. Micromachined Droplet Ejector Arrays for Controlled Ink-jet Printing and Deposition. *Rev. Sci. Instrum.* **2002**, *73*, 2193-2196.

(26) Deegan, R. D.; Bakajin, O.; Dupont, T. F.; Huber, G.; Nagel, S. R.; Witten, T. A. Capillary Flow as the Cause of Stains from Dried Liquid Drops. *Nature* **1997**, *389*, 827-829.

(27) Park, J.; Moon, J. Control of Colloidal Particle Deposit Patterns within Picoliter Droplets Ejected by Ink-jet Printing. *Langmuir* **2006**, *22*, 3506-3513.

(28) Zhang, L.; Maheshwari, S.; Chang, H. C.; Zhu, Y. Evaporative Self-assembly from Complex DNA-colloid Suspensions. *Langmuir* **2008**, *24*, 3911-3917.

(29) Kim, D.; Jeong, S.; Park, B. K.; Moon, J. Direct Writing of Silver Conductive Patterns: Improvement of Film Morphology and Conductance by Controlling Solvent Compositions. *Appl. Phys. Lett.* **2006**, *89*, 264101.

(30) Majumder, M.; Rendall, C. S.; Eukel, J. A.; Wang, J. Y. L.; Behabtu, N.; Pint, C. L.; Liu, T. Y.; Orbaek, A. W.; Mirri, F. J.; Nam, Barron, A. R.; Hauge, R. H.; Schmidt, H. K.; Pasquali, M. Overcoming the "Coffee-stain" Effect by Compositional Marangoni-flow-assisted Drop-drying. *J. Phys. Chem. B* **2012**, *116*, 6536-6542.

(31) Sempels, W.; Dier, R. D.; Mizuno, H.; Hofkens, J.; Vermant, J. Auto-production of Biosurfactants Reverses the Coffee Ring Effect in a Bacterial System. *Nat. Commun.* **2013**, *4*, 1-8.

(32) Still, T.; Yunker, P. J.; Yodh, A. G. Surfactant-induced Marangoni Eddies Alter the Coffee-rings of Evaporating Colloidal Drops. *Langmuir* **2012**, *28*, 4984-4988.

(33) Soltman, D.; Subramanian, V. Inkjet-printed Line Morphologies and Temperature Control of the Coffee Ring Effect. *Langmuir* **2008**, *24*, 2224-2231.

(34) Nagao, Y. A Study on the Plasma-treated Surfaces of MgO (100) and Quartz Substrates by Infrared Multiple-angle Incidence Resolution Spectrometry. *e-J. Surf. Sci. Nanotech.* **2012**, *10*, 229-233.

(35) Lim, Y. Y.; Goh, Y. M.; Liu, C. Q. Surface Treatment for Inkjet Printing onto a PTFE-based Substrate for High Frequency Applications. *Ind. Eng. Chem. Res.* **2013**, *52*, 11564-11574.

(36) Duineveld, P. C. The Stability of Ink-jet Printed Lines of Liquid with Zero Receding Contact Angle on a Homogeneous Substrate. *J. Fluid Mech.* **2003**, *477*, 175.

(37) Modestino, M. A.; Paul, D. K.; Dishari, S.; Petrina, S. A.; Allen, F. I.; Hickner, M. A.; Karan, K.; Segalman, R. A.; Weber, A. Z. Self-Assembly and Transport Limitations in Confined Nafion Films. *Macromolecules* **2013**, *46*, 867-873.

(38) Siroma, Z.; Kaitsubo, R.; Fujiwara, N.; Ioroi, T.; Yamazaki, S. I.; Yasuda, K. Depression of Proton Conductivity in Recast Nafion® Film Measured on Flat Substrate. *J. Power Sources* **2009**, *189*, 994–998.

(39) Paul, D. K.; McCreery, R.; Karan, K. Proton Transport Property in Supported Nafion Nanothin Films by Electrochemical Impedance Spectroscopy. *J. Electrochem. Soc.* **2014**, *161*, 1395-1402.

(40) Paul, D. K.; Karan, K. Conductivity and Wettability Changes of Ultrathin Nafion Films Subjected to Thermal Annealing and Liquid Water Exposure. *J. Phys. Chem. C* **2014**, *118*, 1828-1835.

(41) Paul, D. K.; Fraser, A.; Karan, K. Towards the Understanding of Proton Conduction Mechanism in PEMFC Catalyst Layer: Conductivity of Adsorbed Nafion Films. *Electrochem. Commun.* **2011**, *13*, 774-777.

(42) Paul, D. K.; Karan, K.; Docoslis, A.; Giorgi, J. B.; Pearce, J. Characteristics of Self-Assembly Ultrathin Nafion Films. *Macromolecules* **2013**, *46*, 3461-3475.

(43) Nagao, Y.; Proton Transport Property of Nafion Thin Films on MgO(100) with Anisotropic Molecular Structure. *e-J. Surf. Sci. Nanotech.* **2012**, *10*, 114-116.
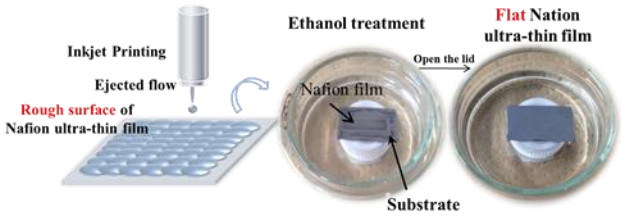
Table of contents (TOC)